Kurdistan Journal of Applied Research (KJAR)
Print-ISSN: 2411-7684 | Electronic-ISSN: 2411-7706

Original Article

Deep Learning Techniques for Early Fault Detection in Bearings: An Intelligent Approach

Omar Mohammed Amin Ali [a*], **Rebin Abdulkareem Hamaamin** [b], **Shahab Wahhab Kareem** [c d]

[a] Department of Information Technology, Chamchamal Technical Institute, Sulaimani Polytechnic University, Sulaymaniyah, Iraq.
[b] Department of Computer Science, College of Sciences, Charmo University, Chamchamal, Sulaymaniyah, Iraq.
[c] Department of Technical Information Systems Engineering, Technical Engineering College, Erbil Polytechnic University, Erbil, Iraq.
[d] Information Technology Department, College of CS and IT, Catholic University, Erbil, Iraq.

Submitted: 1 November 2024
Revised: 11 January 2025
Accepted: 5 February 2025

*** Corresponding Author**:
omar.mohammed@spu.edu.iq

Keywords: Bearing, Deep Learning, Machine learning, Elastic weight consolidation Algorithm, CWRU dataset.

How to cite this paper: O. M. A. Ali, R. A. Hamaamin, S. W. Kareem, "Deep Learning Techniques for Early Fault Detection in Bearings: An Intelligent Approach", KJAR, vol. 10, no. 1, pp: 18-34. June 2025, doi: 10.24017/science.2025.1.2

Abstract: Bearings are essential for spinning machines. An unexpected bearing failure could disrupt production. This study describes a sophisticated method for diagnosing deep groove ball bearing issues. We designed and built an experimental setup to collect precise data in many scenarios, including inner race fault, outer race fault, cage fault, and normal state. Machine learning (ML) and deep learning (DL) algorithms have improved image processing, speech recognition, defect detection, item identification, and medical sciences. Experts anticipate a surge in equipment problems as intelligent machinery becomes more prevalent. Deep learning methods for equipment failure detection and diagnosis have increased steadily. Research papers have used deep learning to study and share open-source and closed source data. The Case Western Reserve University (CWRU) bearing data set identifies abnormalities in machinery bearings. Popularity makes this dataset simple to access. This dataset is 'ideal' for model verification and is widely accepted. This article describes current deep learning research using the CWRU bearing dataset to diagnose machinery faults precisely. Using the CWRU dataset, this article has the potential to be of significant service to future academics who desire to begin their work on the detection and diagnosis of machinery failures. This is our view.This paper focuses on utilizing the CWRU bearing dataset combined with Elastic Weight Consolidation (EWC) algorithm to achieve a notable accuracy of 97.06%. The streamlined approach emphasizes the use of raw data and advanced methodologies, showcasing the significance of achieving high diagnostic accuracy while providing a reliable alternative to conventional fault classification techniques.

1. Introduction

Many production applications currently use electric machines extensively. The expansion of contemporary industries and the quick development of science and technology have resulted in the extensive usage of mechanical equipment in many different applications. However, these devices often work in adverse circumstances, such as high humidity and large loads, which may cause motor issues. This leads not only to expensive maintenance expenses but also to decreased production, significant financial losses, and maybe even a risk to human life. Important parts of industrial systems include rotating machinery and induction motors. The stator, rotor, shaft, and bearings are among the several components that make up these spinning devices [1]. Rolling element bearings, sometimes known as bearings, are vital yet fragile components of machinery. The status of the equipment has a direct impact on its functioning, stability, durability, and efficiency. This includes the occurrence of fractures or other faults in various places under different loads [2]. The rolling element bearing is composed of the inner race, outer race, cage, and ball (REB). The ball bearing systems of the Case Western Reserve University (CWRU) bearing test rig arrangement is shown in figure 1, which also provides a cross-sectional view of the bearing's constituent parts [3, 4]. A number of studies [5, 6] that examined the possibility of induction engine failures found that bearing issues are the most common kind of problem and make up one-third of all defects. These bearings' failure is a major contributor to machine failure, which may result in serious dangers to property and safety as well as, in some cases, machine accidents or fatalities [7]. Due to these features, identifying and evaluating flaws in these REBs has grown in importance as part of engineering and research projects. Without interfering with the production process, it is expected that REBs' condition monitoring and defect detection techniques would provide real-time information on the equipment's operating state. Mechanical vibration signals are also thought to be highly useful and efficient information sources for identifying, locating, and differentiating different types of bearing-related issues [1, 8].

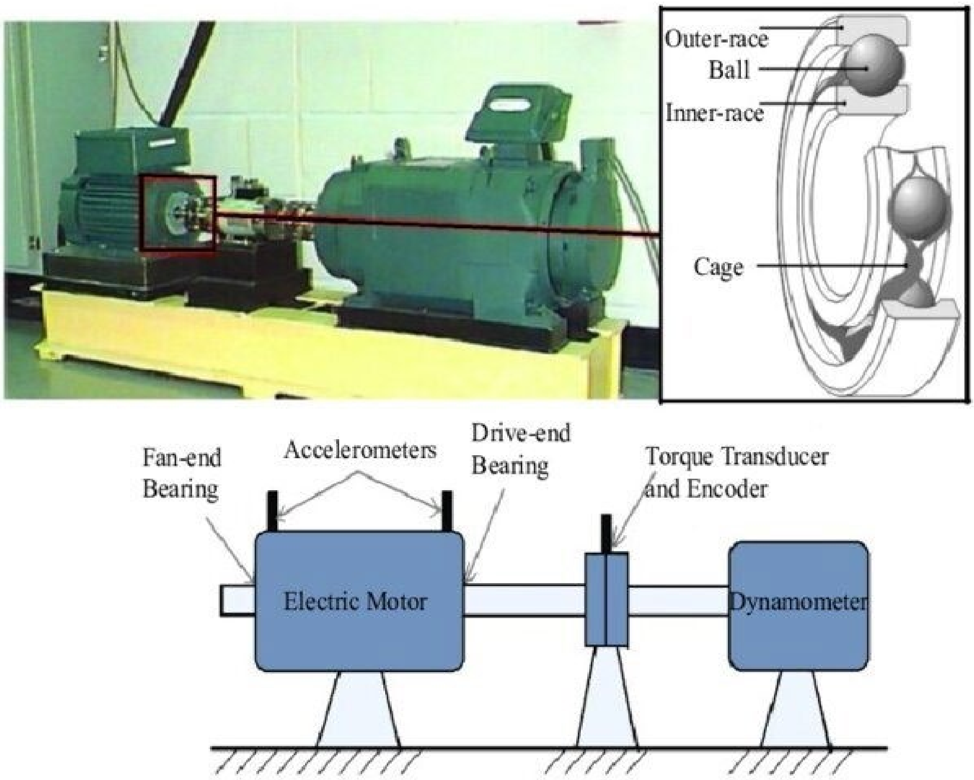

Figure 1: Ball bearing system components are part of the experimental setup of the CWRU bearing test apparatus [4].

The process of identifying bearing problems involves positioning sensors at several locations on the machine. These sensors communicate with the data collection system to provide signals for further analysis [9]. Vibration data collection for the CWRU dataset is shown in figure 2. The quality of the vibration signals gathered, the efficiency of the signal processing and feature extraction techniques, and other factors all affect how effectively defect detection systems work [1]. In the past, we often only performed such equipment maintenance after a fault had occurred. When a posterior maintenance technique is used, unexpected equipment failures often occur, which may cause deaths as well as financial losses [10]. As a result, bearings need to be inspected while the machine is operating. Several machine learning, deep learning, and signal processing methods have been created by researchers to detect and diagnose equipment and REB flaws.

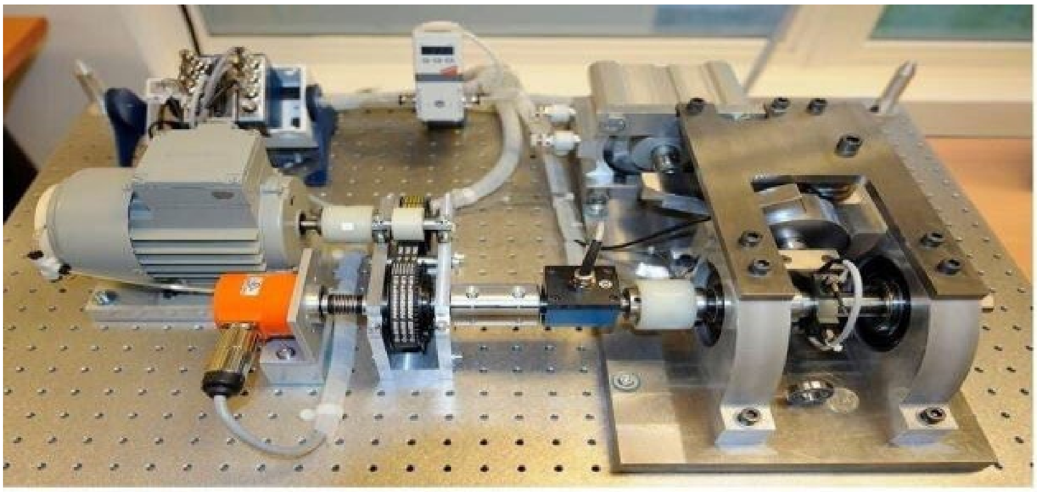

Figure 2: An overview of the PRONOSTIA experimental platform in a format the Paderborn University dataset includes [11].

The increasing reliance on rotating machinery in industrial applications raises concerns over costly and hazardous breakdowns, emphasizing the need for efficient, real-time bearing fault detection. While existing methods are effective to some extent, they struggle with retaining learned knowledge when new fault types are introduced. This limitation hamper's fault diagnosis accuracy. This work introduces Elastic Weight Consolidation (EWC) as a novel technique for bearing fault diagnosis, addressing the issue of catastrophic forgetting. By using EWC, the model retains previously learned knowledge while accurately identifying new fault types. On the CWRU dataset, the EWC-based model achieves a success rate of 97.06%, setting a new benchmark for failure diagnostics and demonstrating its reliability across various fault types.

2. Related work

In order to prevent the leakage of bearing information between splits, Hendriks *et al.* [12] introduced a novel dataset partitioning technique. By using the concept of dividing sets based on fault size instead of load, the authors observed that the leaking of bearing information no longer happened in the measurements of defective bearings. The authors divided fault classification into seven categories, including healthy states and different types of faults at different locations. Their proposed method effectively improved the performance of state-of-the-art deep convolutional networks. These networks initially achieved a classification accuracy of 95% when considering load division but now achieve a more realistic accuracy of 53% when considering fault size division. Abburi *et al.* [13], however, suggested an alternative method of dividing the dataset in order to prevent the leakage of bearing information. Within their proposed division, they exclusively allocate drive-end fault measures for the training set, fan-end fault measurements of sizes 7 and 14 mils for the validation set, and fan-end measurements of size 21 mils for the test sets. The tests used conventional machine learning algorithms, including Random Forest, Naïve Bayes, and Support Vector Machine, to tackle a multi-class issue with three defect categories (inside race, outside race, ball) and a healthy condition. According to the findings, the bearing split performed worse than the random split in all reported metrics (accuracy, precision, macro F1-score, recall). The random split, where the bearing information leaking happened, had better outcomes. The accuracy of the Naive Bayes model decreased from 85.8% to 69.5%. However, as previously said, none of these formulations that include several classes are capable of preventing data leakage from the healthy class, which is why we refrain from utilizing a multi-label method.

While some prior studies have used the CWRU dataset for defect identification and diagnosis using a multi-label method, they have employed various formulations that do not consider the particular issues mentioned in this research. Shen *et al.* [14] examine two multi-class labels that indicate fault type and fault magnitude in the CWRU dataset. Because a single label is used for fault type diagnosis, the problem remains a multi-class issue, assuming that fault types are mutually exclusive. Similarly, Yu *et al.* [15] examine three multi-class labels that correlate to fault magnitude, fault kind, and motor speed, with the exception that the healthy condition is disregarded. This is a multi-class problem that focuses on diagnosing fault types without addressing fault detection. The formulations by Chen *et al.* [16] and Jin *et al.* [17] are the most similar to ours. They use binary labels to represent the three fault types and a healthy state. Additionally, they also include labels for each combination of fault type and size, as described in [12]. Nevertheless, our technique does not require the use of healthy data for training, in contrast to the requirement for healthy state label inclusion. Furthermore, these studies only focus on signals obtained from a single position (either the drive end or fan end) that correspond to problems at that specific position. As a result, the issue of fault localization is not addressed. Significantly, these studies exhibit a distinction from our own in their approach to dividing the information into training and testing divisions. Unfortunately, this divide fails to prevent data leakage [13], whether it be at the segmentation level or the bearing level. These leakages mostly result in excessively optimistic outcomes with virtually perfect accuracy, making it impossible to accurately assess their effectiveness. None of these studies consider the use of fan end signals as negative samples for detecting defects at the drive end, and vice versa. As far as we know, our research is the only one that has used a multi-label approach on the CWRU dataset to tackle issues like bearing data leakage and imbalance in the healthy class. This approach helps to better align the problem with real-world conditions and ensures accurate evaluation of the model.

Altogether, the cited papers enhance the progress of fault diagnosis and prognosis of rotating machinery, bearings, and industrial equipment with the help of machine learning, deep learning, and hybrid optimization. A number of these works Residual Diagnosis towards the intelligent fault detection frameworks using the time-frequency analysis with self-attention mechanism and neural network for the purpose of fault detection, classification, and rolling bearing remaining useful life estimation. For example, Rajabi *et al.* [18] and Yang *et al.* [19] put forward the new idea of permutation entropy-based neuro-fuzzy models and indexes of performance degradation for enhancing the fault detection rate, and Liu and Fan [20] introduced the new built multistage model of adaptive adjudging which has taken the three-source varying into consideration. Literatures like Saha *et al.* [21] and Ding *et al.* [22] focus on the use of transformer-based architectures and self-attention mechanism for better fault feature identification and diagnosis of the rolling bearings. Furthermore, Lu *et al.* [23], Zhang *et al* [24], and Alonso-Gonzalez *et al.* [25] present the use of deep learning techniques such as stacked denoising autoencoder and envelope analysis for signal processing **in** diagnosis of faults. Some of the works, which have explored Convolutional Neural Network - Long Short-Term Memory approaches include Tian *et al*. [26], Sun and Zhao [27], and Ince *et al.* [28] that aimed at enhancing the classification capabilities when operating under different conditions through learning from hybrid models and self-organizing neural networks. Other similar studies Toma *et al.* [29], Yang *et al*. [30] uses conditional Generative Adversarial Networks and Two-Dimensional Convolutional Neural Networks to improve fault recognition with a few training samples while Patil *et al*. [31], Barcelos & Marques Cardoso [32] uses harmonic spectrum analysis and deep learning approach to diagnose faults from current signals. Also, the knowledge of Munir *et al.* [33] and Xie *et al*. [34] is helpful as the authors used the Gated Recurrent Units - Long Short-Term Memory networks and multi-layer perceptron hybrid in the identification of software defects and bearings faults. The current year's works contain Li *et al*. [35], Xia *et al.* [36], and Saberi *et al.* [37] in that they employ federated learning, Light GBM models, and recursive feature to enhance the scalability of fault detection under different working conditions. At last, in Kiranyaz *et al*. [38], the authors disclose how the blind domain adaptation can be used in predictive maintenance by presenting a zero-shot domain transition method for motor health monitoring.

These papers together show a development of artificial intelligence based methods for the diagnosis of industrial faults to support real-time prognosis and reliability estimation of industrial systems by deep learning feature extraction and adaptive optimization technique.

3. Materials and Methods

The methodology for fault detection in the bearing dataset, as well as the visualization process. Figure 3 graphically depicts the neural network framework that this study utilized. To apply EWC algorithm within the neural network framework for fault classification and visualization using relevance maps, we preprocessed the bearing dataset to extract pertinent characteristics from the signal data. The following subsections provide an extensive description of these techniques.

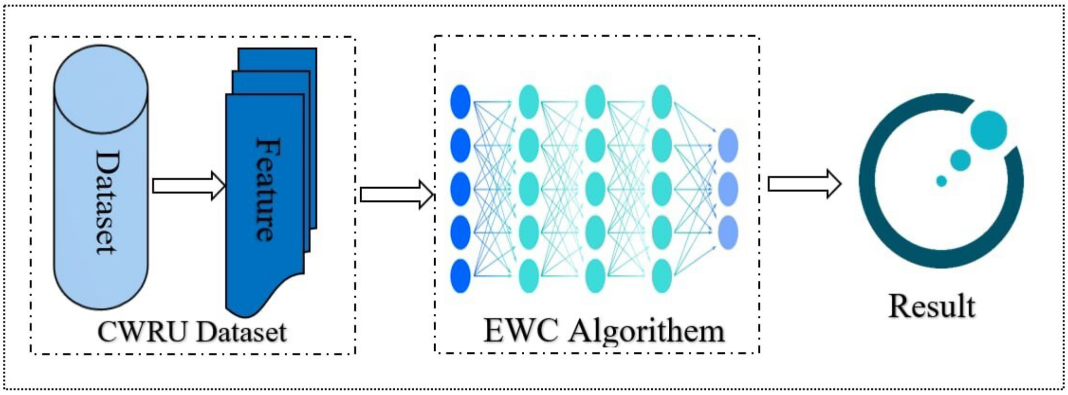

Figure 3: EWC-based fault detection methodology diagram.

Figure 4 illustrates the division of the paper's overall methodology into several stages. All stages are explained below. In bearing fault detection, the terms "inner," "outer," "ball," and "normal" refer to different, conditions or locations of faults within a bearing:

- **Inner Race Fault:** This type of fault occurs in the bearing's inner race. The inner race is the inner ring that rotates along with the shaft. Faults here can cause high-frequency vibrations due to the constant contact between the balls or rollers and the damaged inner surface.
- **Outer Race Fault:** This fault is located on the bearing's outer race, which is the outer ring that typically remains stationary in the bearing housing. Faults on the outer race produce distinct vibration patterns as the balls or rollers pass over the damaged area.
- **Ball Fault:** This refers to a fault in the rolling elements themselves, such as the bearing's balls or rollers. A defect in the ball can lead to vibrations when it contacts the races (both inner and outer), affecting the overall performance of the bearing.
- **Normal (Healthy):** This condition refers to a bearing in good working order with no detectable faults. The vibrations from a normal bearing will be minimal and consistent, as there are no defects in the races or rolling elements. In fault detection, the goal is to identify these specific types of faults based on the vibration signals or other data collected from the bearing. We can analyze each type of fault's unique vibration signature to ascertain its presence and severity.

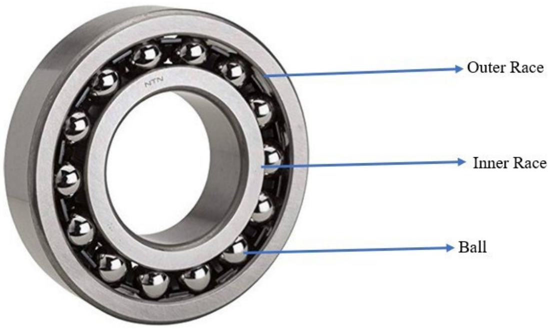

Figure 4: Components of a bearing (typical bearing faults).

3.1. Dataset CWRU

The CWRU dataset is widely used, freely available, and readily accessible. The dataset, which includes recorded data on both normal and problematic bearings, is stored and accessed on the CWRU website. Both standard bearings and bearings with single-point failures in the drive-end (DE) and fan-end (FE) regions are included in the database. We use the dataset as a fundamental dataset [2] and as a benchmark [39] to evaluate the effectiveness of various machine learning and deep learning approaches. The procedure for obtaining the Case Western Reserve University dataset using a bearing test rig design is shown in figure 1. The system consists of a dynamometer, a torque transducer, a 2-horsepower Reliance electric induction motor, and control electronics that are not seen in the photo. The test bearings provide support for the motor shaft. The torque for the shaft is produced by a dynamometer and an electronic control system. We intentionally introduced flaws in the inner and outer races of the REBs. After that, the test rig repaired all of the troublesome bearings. Using electro discharge machining, we manufactured single-point flaws in the test bearings with diameters of 7, 14, 21, 28, and 40 mils. 0.001 inches is equal to one mil. We utilized Svenska Kullagerfabriken bearings for faults with diameters of 7, 14, and 21 mil, and Nitto Toyo Needle bearings of similar quality for faults with dimensions of 28 and 40 mil. The fault depth was consistent at 0.011 inches for all the bearings except for the inner-race defective bearing (diameter: 0.028 inches), the outer-race faulty bearing (diameter: 0.040 inches), and the ball bearing fault (diameter: 0.028 inches). The 0.050-inch fault depth is shared by the 0.028-inch inner-race and 0.040-inch outer-race defective bearings. Furthermore, we have determined that the ball-bearing flaw is 0.150 inches deep and has a diameter of 0.028 inches [4].

The dataset consists of 161 records from four classes: 48k normal baseline, 48k drive-end fault, 12k drive-end fault, and 12k fan-end fault. Datasets for inner-race, outer-race, and ball bearing difficulties are included in each category. We classify the outer race faults into three groups based on their relative locations to the load zone: "centered" faults (fault at 6 o'clock), "orthogonal" faults (fault at 3 o'clock), and "opposite" faults (fault at 12 o'clock). There is a pattern to the data file names: the bearing loads are indicated by the last number, the fault diameters are represented by the following three numbers, and the fault location is indicated by the first letter. For example, information on a ball bearing problem may be found in data file 'B007_0.'. The bearing develops a 0.007-inch-diameter flaw while it is operating at a motor load of zero horsepower. Details on an outer-race flaw of 0.014 inches are included in the data file "OR014@6_1.". The failure happened at six o'clock after we centered the weight. We saw the problem when the system operated with a motor load of one horsepower [4]. This dataset is used in bearing defect diagnostics [40]. Important parts of the test rig include a load motor, a test module, a driving motor, and a torque measuring shaft. The mechanical setup of the experimental equipment used for the Paderborn University dataset. High-resolution vibration data from testing on 26 sets of damaged bearings and six sets of undamaged bearings make up the Paderborn University bearing dataset. In order to simulate actual degradation, twelve of the twenty-six purposefully damaged bearing sets underwent accelerated life testing [41, 42].

This dataset is publicly accessible due to the efforts of CWRU. In this research used the CWRU dataset to evaluate the proposed approach. The experimental setup utilized by CWRU to investigate issues relating to ball bearings is shown in figure 5. Three accelerometers were utilized to detect vibrations. At the hour mark, we mounted the accelerometers on the housings for the DE and FE. The Svenska Kullagerfabriken deep-groove ball bearings, including the 6205-2RS and 6203-2RS JEM models, were used by the DE and FE.

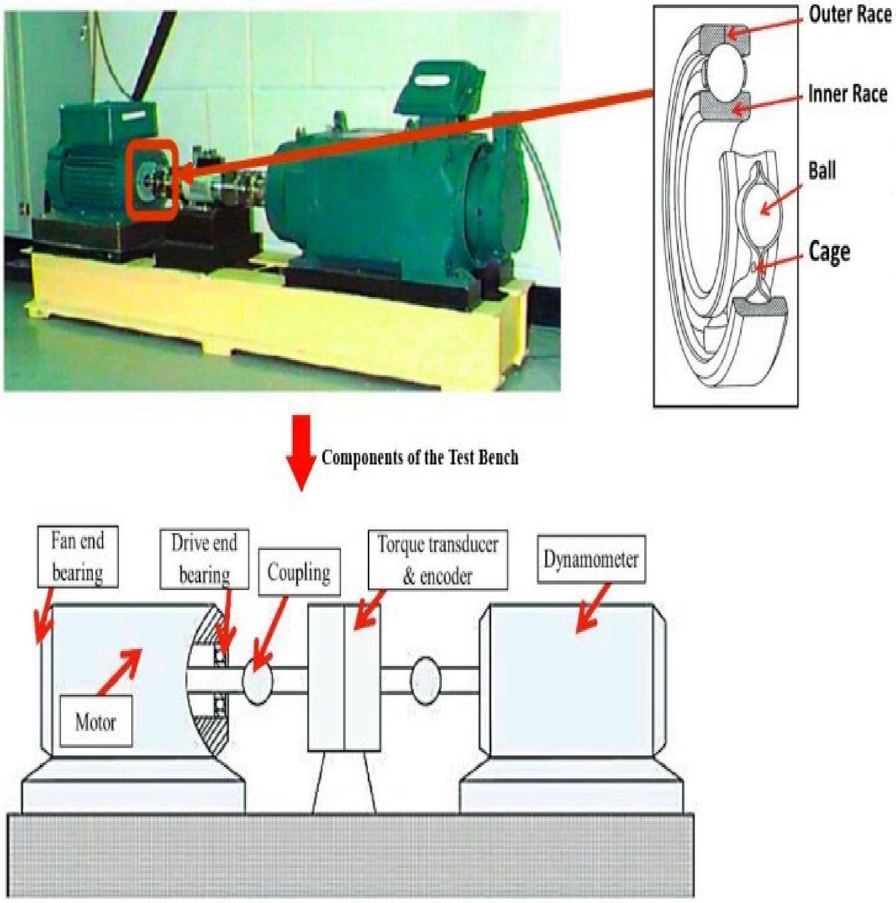

Figure 5: CWRU motor experimental rig [11].

Table 1: CWRU Bearing Dataset Description [2, 43].

Fault Type	Fault Diameter (Inch)	Fault Position Relative to Load Zone	Fault Labels	Load (hp) 0	1	2
Normal	0	-	N	243,938	485,643	485,643
Ball	0.007 0.014 0.021	-	7_BA 14_BA 21_BA	243,538 249,146 243,938	486,804 487,384 487,384	488,545 486,804 491,446
Inner Race	0.007 0.014 0.021	-	7_IR 14_IR 21_IR	243,938 63,788 244,339	485,643 487,964 491,446	485,643 485,063 486,804
Outer Race	0.007 0.014 0.021	@6:00 @3:00 @12:00 @6:00 @6:00 @3:00 @12:00	7_OR1 7_OR2 7_OR3 14_OR1 21_OR1 21_OR2 21_OR3	244,739 124,602 129,969 245,140 246,342 128,663 130,549	486,804 485,643 483,323 486,804 487,964 487,384 486,804	487,964 486,224 484483 488,545 489,125 484,483 486,224
		Total Data Points		**2,782,629**	**6,816,994**	**6,816,996**

Table 1 lists the number of data points for each type, size, and location of fault under three distinct load scenarios. These counts show significant differences. The dataset typically has 243,938 data points when there is no load (0 hp). The dataset does, however, indicate a decline to 243,538 data points in the instance of a ball defect with a diameter of 0.007 inches. The dataset's overall number of data points increases dramatically with load, indicating its magnitude and potential for extensive model training and assessment. To enable exact detection and investigation, we use fault labels to represent the kind, extent, and location of the problem. Our study aims to assess the performance of several machine learning models, including both conventional methods and neural networks, in accurately detecting bearing problems using this dataset. Our goal is to improve fault diagnosis processes and gain a deeper understanding of how load variations and specific problems affect diagnostic accuracy using an integrated approach.

3.2. EWC Algorithm

The study extracted specific features from a dataset to aid in fault identification and prediction. The following nine features were calculated for this purpose: minimum, maximum, mean, standard deviation, root mean square, skewness, kurtosis, crest factor, and form factor. These features were computed for time segments containing 2048 data points, corresponding to 0.04 seconds of signal at a sampling frequency of 48 kHz. This was the best strategy in achieving the objective of identifying the right characteristics of the signals of the fault. When it comes to fault detection in bearings, we use the EWC algorithm to handle the problem of continual learning, which mainly comprises of catastrophic forgetting. To improve the performance of the fault detection system in capturing essential information about previous states of the bearing as well as adapting to new data that reflects different fault conditions, we incorporate the EWC method in the modelling process. With regards to bearings, which are organizational parts of rotating mechanisms, the bearings are apt to be put through several running conditions that cause different types of defects. The objective is to create a classifier that can identify these kinds of faults when they occur in the future but, at the same time, does not forget the kinds of faults it has seen in the past. In this framework, one can further train this model on different fault conditions by applying the EWC algorithm that allows the model to recognize earlier faults while at the same time training from other faults.

3.2.1. Implementing EWC for Bearing Fault Detection Steps

- **Initial Training on Baseline Data:** We first then train our chosen neural network model on a simple baseline data set that comprises both healthy bearing data and data from the first type of fault. In the model's diagnostic phase, it is trained to differentiate between normal and faulty states through parameters like max, min, mean, dev, root mean square, skewness, kurtosis, crest factor, and form factor. Skewness and kurtosis were selected because they provide valuable insights into the asymmetry and peakiness of the vibration signal, which are crucial for detecting abnormalities that may not be captured by other traditional statistical features. Skewness helps identify deviations from a normal distribution in the signal, which can point to irregular fault behavior. Kurtosis, on the other hand, indicates the presence of sharp peaks in the vibration signal, which are often associated with mechanical faults like cracks or wear in bearings.
- **Computation of Fisher Information Matrix:** Once having learned on the baseline data set, we compute the Fisher Information Matrix (FIM) for the parameters of the tuned model. The FIM highlights the parameters used for defining the first failure conditions, making sure that these parameters are preserved during subsequent training.
- **Sequential Learning with EWC Regularization:** The EWC algorithm retrains the model when new data in the form of different fault conditions are acquired by the model. We add the EWC regularization term to the loss function to confine the drastic change of learned parameters detected by the FIM. This is done in a way that enables the model to

update new fault patterns while it is capable of recognizing other faults that it has been trained on earlier.

- **Ongoing Model Evaluation:** During the training phase, the model is tested through the use of the current as well as the previous database or data so as to test its efficiency in addressing all the possible fault conditions. That is how EWC contributes to the best/aversion of the enhanced rate of new faults with the rates of knowledge retention. Therefore, applying the EWC algorithm adds to the methodology the ability to improve its performance in the search for faults as well as guard against the threats posed by the process of continual learning. This approach ensures that we have developed a robust model that works in real-life applications where the condition of the bearing changes with time and may emerge new faults. The flowchart outlines the process for bearing fault detection using the proposed model with the EWC algorithm. It starts with the CWRU dataset, followed by feature extraction to derive key signal characteristics. Next, the hyperparameters are adjusted to optimize the model. Afterward, model testing is performed to evaluate its performance, followed by model training to refine its fault detection capabilities. The resulting accuracy is assessed to determine the model's effectiveness. Finally, the proposed model incorporating the EWC algorithm is implemented to enhance continual learning and fault detection. The process concludes with the end. Figure 6 illustrates this sequence.

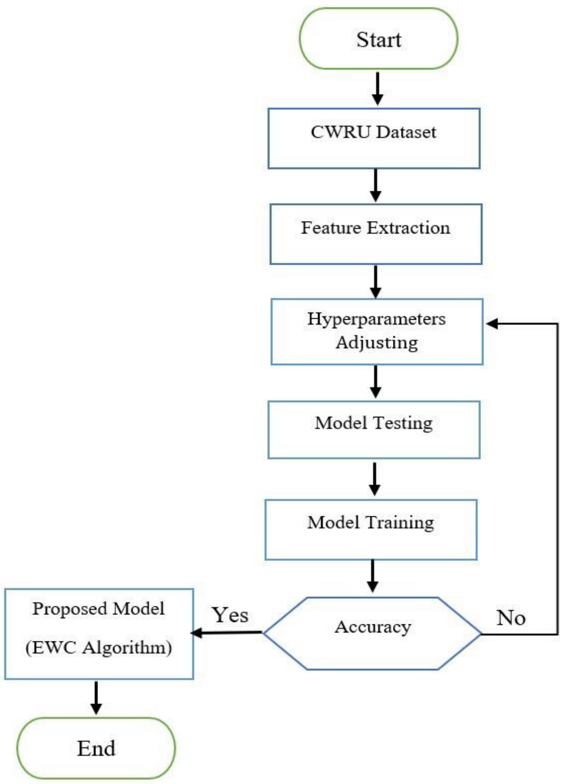

Figure 6: Flow chart for methodology.

3.3. Evaluation Metrics

3.3.1. Accuracy

Accuracy is a fundamental metric for evaluating the success of classification algorithms. Accuracy is defined as the proportion of accurate forecasts to the total number of predictions made. You can determine the calculation using the following equation (1).

$$\text{Accuracy} = \frac{TP + TN}{TP + TN + FP + FN} \tag{1}$$

3.3.2. Precision

Precision can be defined as the proportion of correctly predicted true values to the total number of expected true values shown in equation (2).

$$\text{Precision} = \frac{TP}{TP + FP} \tag{2}$$

3.3.3. Recall

Recall is a statistical measure that quantifies the proportion of correctly identified positive cases (true positives) relative to the total number of positive cases, including both correctly identified and incorrectly missed cases (false negatives). Accurate identification and classification of the actual positive cases determine the real positive rate of the model. Use the following in equation (3) to determine the calculation:

$$Recall = \frac{TP}{TP + FN} \tag{3}$$

3.3.4. F1 Score

When comparing two models with high recall but poor accuracy, or vice versa, it becomes challenging to determine which one is superior. In this scenario, adding the F1 score as a third element allows for a meaningful comparison to be shown in equation (4).

$$\text{F1} = 2 * \frac{Precision * Recall}{Precision + Recall} \tag{4}$$

True Positive (TP) denotes the quantity of instances in which the model accurately identifies the positive class. True Negative (TN) denotes the instances in which the model accurately identifies the negative class. A false positive (FP), or "Type I error," arises when the model erroneously classifies a negative instance as belonging to the positive class. A false negative (FN) occurs when the model does not identify a positive instance as belonging to the positive class. Figure 7 illustrates the confusion matrix, which serves as an evaluation method for both binary and multiclass classification.

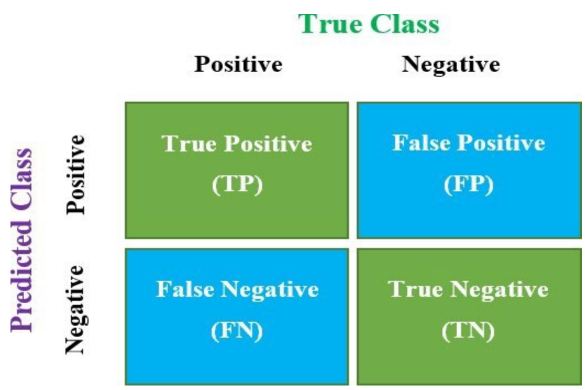

Figure 7: Confusion matrix.

4. Results

That is why we decided to perform the full set of experiments to illustrate the applicability of the suggested model and check that the elastic EWC method is effective on the CWRU dataset. The aim was to fine-tune the EWC algorithm with significant parameters in an effort to achieve the most successful results. In our technique, we started our training process with the basic training of 50 epochs. Any subsequent extension had to be measured against this; to this end, this session served as the control point. After the first run, we continued with enhancing the number of epochs up to 100 and then to 150 in the following runs. The objective was to find out the effects of modifying the number of training cycles on the ability of the model to generalize as well as to recognize defect patterns in the data. Aside from these changes, the learning rate was adjusted and controlled, and a range of values from 0.001 to 0.003 was used. By this we can also mean how fast the adjustment of the model is when the new input is given, and this is referred to as the learning rate. Hence, the learning rate used also needs to be adjusted to the best performance possible.

The following are some of the observations obtained from the experimentation results shown in figure 8. We settled on a learning rate of 0. As discussed in the earlier section, while tuning the system for the first time, 002 always offered optimal results. Inspired by this, we performed additional experiments, including this chosen learning rate, on various epoch configurations.

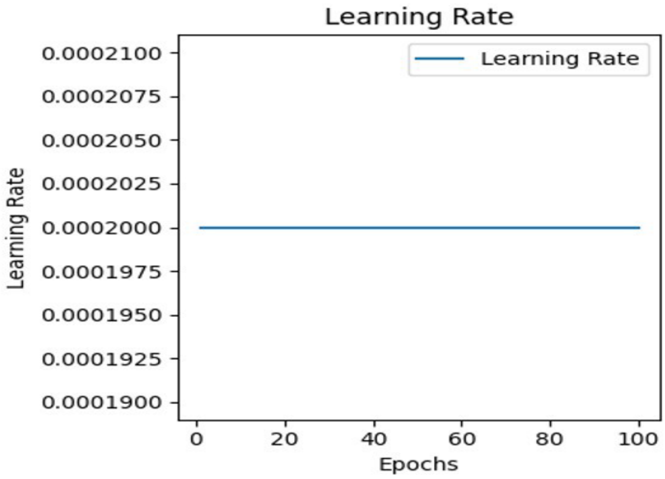

Figure 8: Learning rate optimization for proposed method.

These endeavors were paid off when it was found that the model yielded the best results with a particular setup of 100 epochs with a learning rate of 0.002. Such a setup, as indicated in figure 9 (a)Training loss and (b) test accuracy across bellow, made it possible for the model to term an accuracy level of 97.06%. This result not only exhibits the proposed tuning process as useful for deriving more accurate emotion recognition models but also shows a marked improvement over prior technique. The level of achieved accuracy of 97. The other 06% amplifies the effectiveness of the proposed approach in solving the classification of faults according to the CWRU dataset

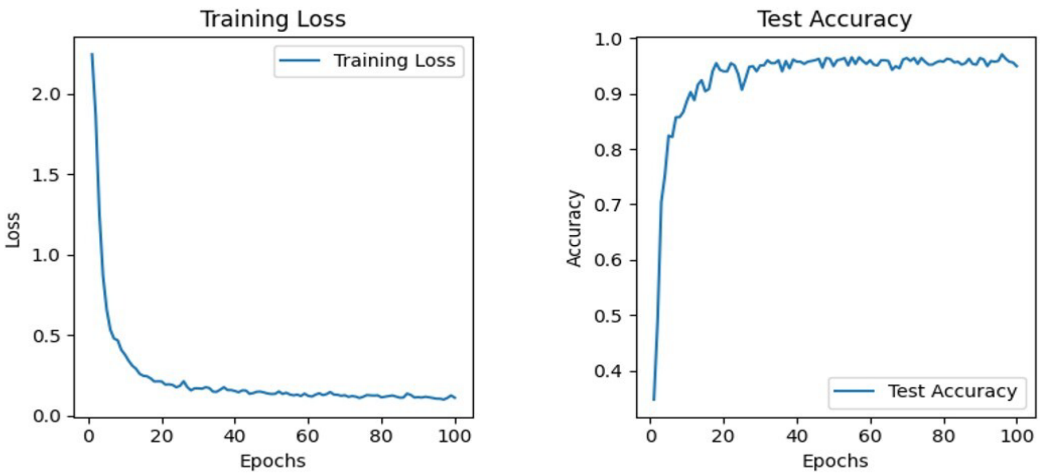

(a) (b)

Figure 9: (a) Training loss and (b) test accuracy across epochs.

A comprehensive report on the categorization of each fault type using the EWC Algorithm is included in table 2, which includes metrics for Precision, Recall, and F1-Score. Notable faults that achieved perfect scores (precision, recall, and F1 score of 1.0) are IR_014_1, IR_021_1, and OR_007_1. The model exhibits exceptional performance across all kinds of defects. Because of this, it seems the EWC model may accurately identify some types of defects. A comprehensive report on the categorization of each fault type using the EWC Algorithm is included in table 2, which includes metrics for Precision, Recall, and F1-Score. Notable faults that achieved perfect scores (precision, recall, and F1 score of 1.0) are IR_014_1, IR_021_1, and OR_007_1. The model exhibits exceptional performance across all kinds of defects. Because of this, it seems the EWC model may accurately identify some types of defects.

Table 2: Classification report of EWC algorithm.

SN	Fault Types	Precision	Recall	F1-Score
01	Ball_007_1	0.973684	0.986667	0.980132
02	Ball_014_1	0.970149	0.866667	0.915493
03	Ball_021_1	0.985294	0.893333	0.937063
04	IR_007_1	0.986842	1.000000	0.993377
05	IR_014_1	1.000000	1.000000	1.000000
06	IR_021_1	1.000000	1.000000	1.000000
07	Normal_1	0.974026	1.000000	0.986842
08	OR_007_1	1.000000	1.000000	1.000000
09	OR_014_1	0.848837	0.973333	0.906832
10	OR_021_1	0.986667	0.986667	0.986667

The EWC model's overall classification performance indicators are shown in table 3. The model is resilient and has balanced prediction performance across multiple fault classes, as shown by the accuracy of 97.07%, high precision of 97.25%, recall of 97.07%, and F1-Score of 97.06%.

Table 3: The model analysis is proposed for all metrics.

SN	Metric	Classification %
01	Accuracy	0.9706666
02	Precision	0.9725499
03	Recall	0.9706667
04	F1-Score	0.9706406

5. Discussion

A confusion matrix is a tabular form that accurately determines how well a machine learning model is performing in terms of classification, especially when the real values have been predetermined. Figure 10 gives the results of the classification performance through a confusion matrix, which takes detailed results of the classification for many categories of faults. The matrix exhibits the ability of the model in predicting the actual labels, where all diagonal cells represent the number of instances that were correctly classified, while all the other cells are the instances that were misclassified. Additionally, the total scores of the predictions within the testing occurrences are compared to the total testing occurrences as well as the ratio they present as another criterion of measuring prediction precision of the model. When clearly presented, the confusion matrix also indicates the areas of the model that should be further improved on for the classification of faults.

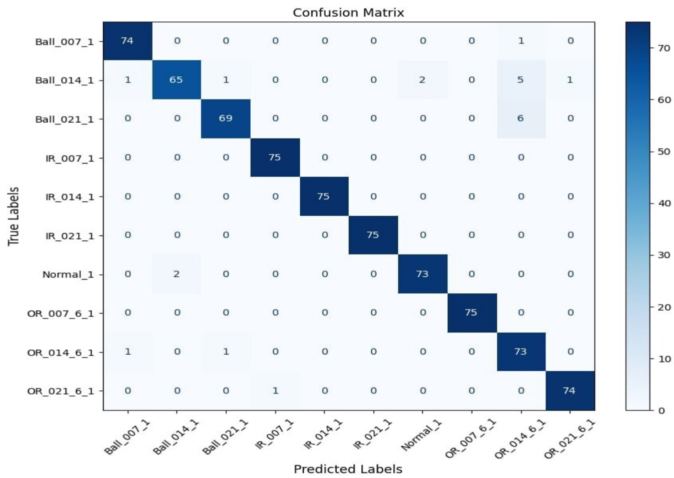

Figure 10: Confusion matrix for fault classification performance.

The EWC Algorithm shows a high level of competence to effectively detect fault types, according to tables 2 and 3. Classes like IR_014_1 and OR_007_1 have excellent accuracy, recall, and F1-Score, indicating that the model can reliably identify these errors without misclassification. To achieve equal sensitivity across all fault types, more tweaking may be necessary, nevertheless, since Ball_014_1 and OR_014_1 had somewhat lower scores. Table 3's total metrics confirm the model's high degree of generalizability with an accuracy of 97.07%. In figure 11 (a) Precision, (b) Recall, (c) F1 Score and (d) chart per class. we can see the metrics presented in tables 2 and 3 compared against one another for each defect category: Precision, Recall, and F1-Score. Supporting the model's dependability in fault categorization, this chart illustrates its constant performance across diverse fault kinds. By highlighting the EWC model's efficacy and revealing avenues for improvement, small changes in individual categories reveal places where more tuning might improve overall accuracy and recall.

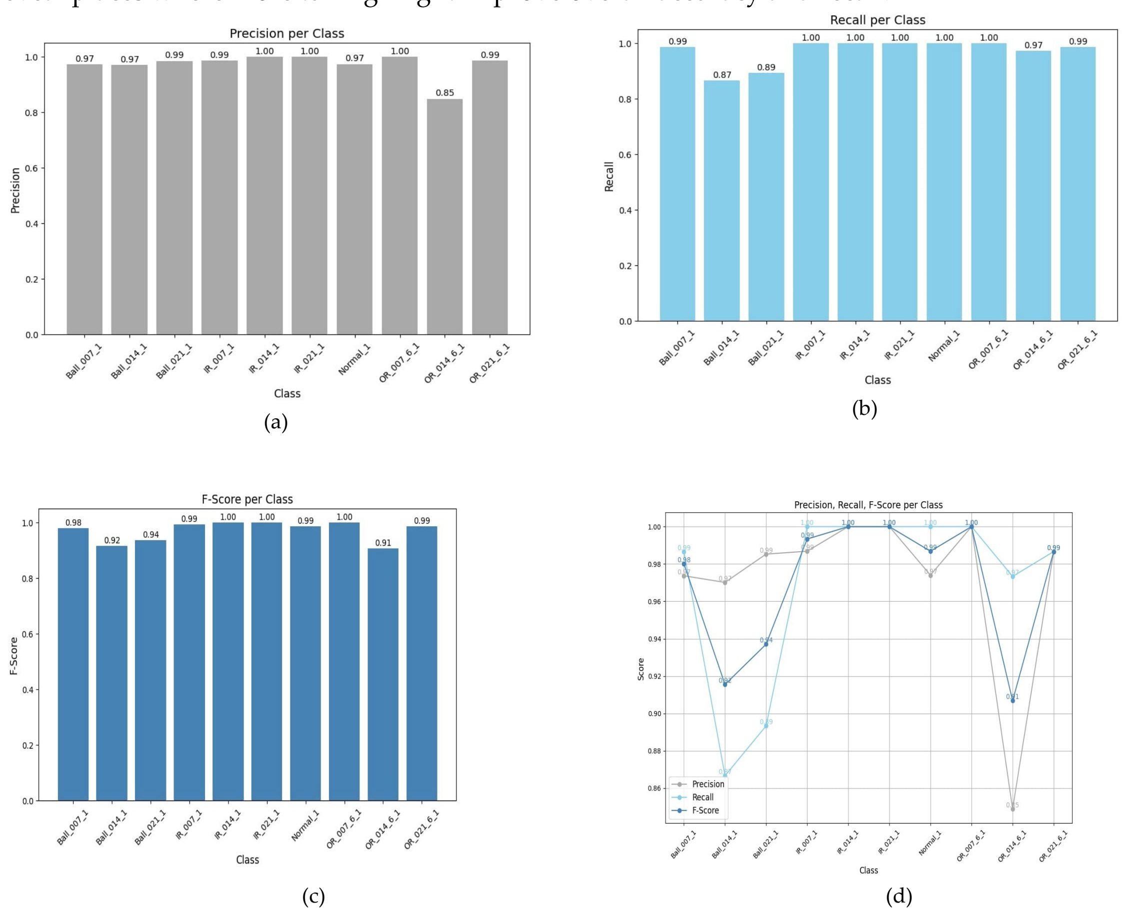

Figure 11: (a) Precision, (b) Recall and (c) F1 Score (d) chart per class.

Finally, table 4 displays the results of a performance comparison between the suggested system and a few cutting-edge methods.

Table 4: Comparison with contemporary state of the art and pertinent studies.

Ref	Techniques	Database	Accuracy %
[44]	DBN	CWRU	84.2
[45]	DNN	CWRU	94.4
[46]	DWAE-ELM	CWRU	95.20
[47]	WDCNN	CWRU	95.9
[48]	GAN-SDEA	CWRU	96
Proposed	**EWC**	**CWRU**	**97.06**

5.1. Practical Diagnostic Performance Under 1-2 hp and 2-1 hp Load Conditions

To assess the practical robustness and generalization ability of the proposed EWC-based fault diagnostic system, we conducted experimental testing under variable load conditions using a practical bearing fault data acquisition platform. A vibration sensor was placed on the DE of the bearing to collect signals under both intact and faulty conditions. The motor was operated at a load of 1-2 hp and 2-1, simulating real-world variations in operating conditions. In these practical tests, the EWC algorithm achieved a fault classification accuracy of 92.03 and 90.64, which, while lower than the 97.6% accuracy achieved under controlled experimental conditions, still demonstrates a strong capability to identify faults. The reduction in accuracy highlights the challenges posed by real-world variability, such as noise and signal inconsistencies, reinforcing the importance of further optimizing the model for practical deployment in complex environments. Illustrates the diagnostic performance of under controlled conditions and practical testing at figure 12 (a) 1-2 hp and (b) 2-1 hp loads. the diagnostic performance of the EWC algorithm under controlled conditions and practical testing with a 1-2 hp and 2-1 hp load. In figure 13, the chart highlights the reduction in accuracy when transitioning from controlled experimental conditions to real-world scenarios, emphasizing the challenges posed by practical variability in fault detection tasks.

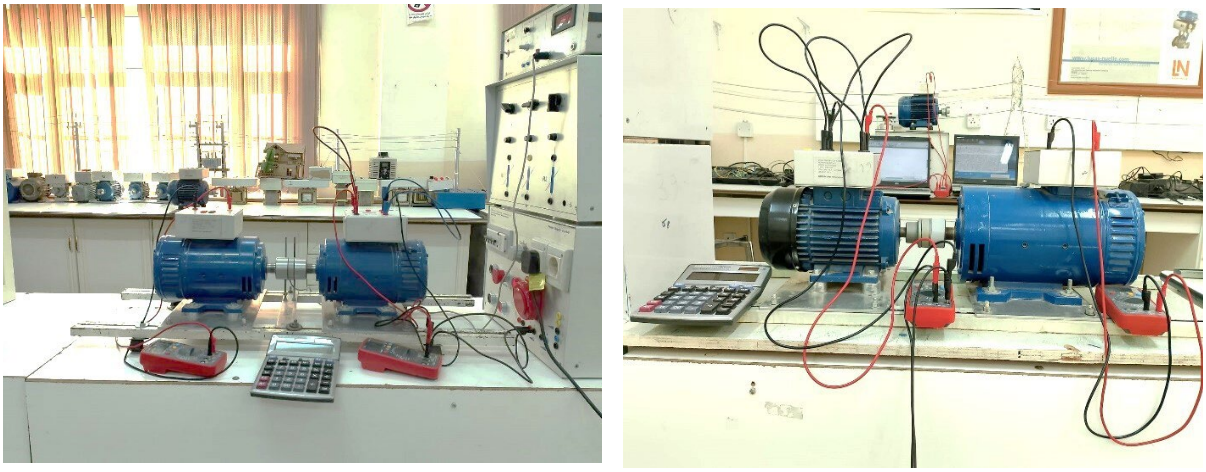

(a) (b)

Figure 12: illustrates the diagnostic performance of under controlled conditions and practical testing at (a) 1-2 hp and (b) 2-1 hp loads.

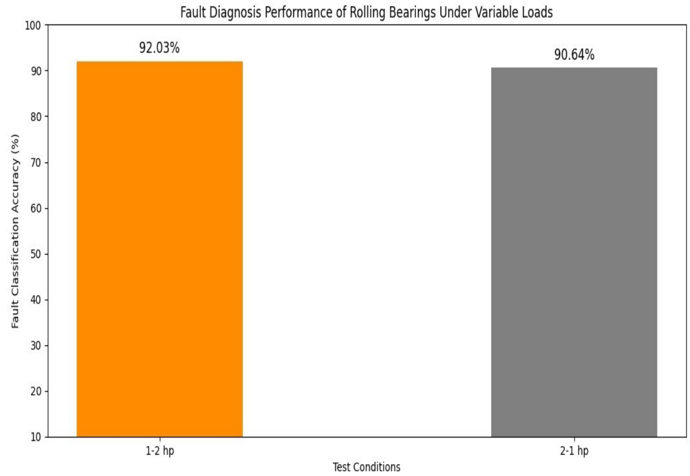

Figure 13: Practical rolling bearing fault data acquisition platform.

6. Conclusions

This paper presents the development of a data-driven intelligent fault diagnostic system for the early identification of faults in deep groove ball bearings. We examined the experimental data to distinguish the defective bearing from the intact one, taking into account the extent of the fault. Also, obtained data during testing under quiet conditions and securely placed the base to prevent any self-induced vibrations. The vibration analyzer's default computational tool transformed the picture data into numerical data. This study presents a method for effectively categorizing defects related to bearings. We should emphasize that the particular dataset under examination and its attributes can greatly influence a classifier's effectiveness. Although some classifiers may exhibit subpar performance on a specific dataset, the ongoing rapid advancement in computer technology ensures that DL models will remain resilient and appealing instruments in machinery problem detection and diagnostic systems. This is the first research to use the EWC algorithm to identify rotating equipment failures in the CWRU dataset. Deep learning helped the EWC algorithm classify the CWRU dataset with 97.6% accuracy. This proves that the EWC algorithm can handle complex defect detection scenarios that need accuracy and knowledge preservation. EWC's success raises the standard for CWRU dataset fault diagnostics.

The key limitation of this study is the lack of access to large industrial machinery for real-world testing. This restricts the validation of the proposed approach to experimental datasets, such as the CWRU dataset, and may not fully represent the challenges and variability encountered in actual industrial environments. Future research should focus on testing the proposed method on larger machines and in operational settings to validate its robustness and scalability. Such efforts would help bridge the gap between experimental studies and practical applications, further advancing the reliability of data-driven fault diagnostic systems.

Acknowledgments: Chamchamal Technical Institute of Sulaimani Polytechnic University, which helped us by providing laboratories for the Technic Electrical Department to conduct the practical part of this research.

Author contributions: Omar Mohammed Amin Ali: Conceptualization, Investigation, Methodology, Project administration. **Rebin Abdulkareem Hamaamin:** Data curation, Resources, Software, Supervision, Validation, Visualization, Writing – original draft, **Shahab Wahhab Kareem:** Writing – review & editing.

Data availability: Data will be available upon reasonable request.

Conflicts of interest: The authors declare that they have no known competing financial interests or personal relationships that could have appeared to influence the work reported in this paper.

Funding: The authors did not receive support from any organization for the submitted work.

Reference

[1] A. Boudiaf, A. Moussaoui, A. Dahane, and I. Atoui, "A comparative study of various methods of bearing faults diagnosis using the case western reserve university data," *Journal of Failure Analysis and Prevention*, vol. 16, no. 2, pp. 271–284, Apr. 2016. https://doi.org/10.1007/s11668-016-0080-7

[2] S. Zhang, S. Zhang, B. Wang, and T. G. Habetler, "Deep learning algorithms for bearing fault diagnostics—A comprehensive review," *IEEE Access*, vol. 8, pp. 29857–29881, 2020. https://doi.org/10.1109/ACCESS.2020.2972859

[3] S.-Y. Li and K.-R. Gu, "Smart fault-detection machine for ball-bearing system with chaotic mapping strategy," *Sensors*, vol. 19, no. 9, p. 2178, 2019. https://doi.org/10.3390/s19092178

[4] D. Neupane, Y. Kim, and J. Seok, "Bearing fault detection using scalogram and switchable normalization-based CNN (SN-CNN)," *IEEE Access*, vol. 9, pp. 88151–88166, 2021. https://doi.org/10.1109/ACCESS.2021.3089698

[5] R. N. Bell, D. W. McWilliams, P. O'Donnell, C. Singh, and S. J. Wells, "Report of large motor reliability survey of industrial and commercial installations, part I," *IEEE Transactions on Industry Applications*, vol. IA-21, no. 4, pp. 853–864, Apr. 1985. https://doi.org/10.1109/TIA.1985.349532

[6] R. N. Bell, C. R. Heising, P. O'Donnell, S. J. Wells, and C. Singh, "Report of large motor reliability survey of industrial and commercial installations, part II," *IEEE Transactions on Industry Applications*, vol. IA-21, no. 4, pp. 865–872, Jan. 1985. https://doi.org/10.1109/TIA.1985.349533

[7] W. Huang, J. Cheng, and Y. Yang, "Rolling bearing fault diagnosis and performance degradation assessment under variable operation conditions based on nuisance attribute projection," *Mechanical Systems and Signal Processing* vol. 114, pp. 165–188, Jan. 2019. https://doi.org/10.1016/j.ymssp.2018.05.015

[8] M. S. Safizadeh and S. K. Latifi, "Using multi-sensor data fusion for vibration fault diagnosis of rolling element bearings by accelerometer and load cell," *Information Fusion*, vol. 18, pp. 1–8, Jul. 2014. https://doi.org/10.1016/j.inffus.2013.10.002

[9] R. A. Patel and B. R. Bhalja, "Condition monitoring and fault diagnosis of induction motor using support vector machine," *Electric Power Components and Systems. Syst.*, vol. 44, no. 6, pp. 683–692, Apr. 2016. http://dx.doi.org/10.1080/15325008.2015.1131762

[10] C. Sun, Z. Zhang, Z. He, Z. Shen, and B. Chen, "Manifold learning-based subspace distance for machinery damage assessment," *Mechanical Systems and Signal Processing*, vols. 70–71, pp. 637–649, Mar. 2016. https://doi.org/10.1016/j.ymssp.2015.09.032

[11] D. Neupane and J. Seok, "Bearing fault detection and diagnosis using case western reserve university dataset with deep learning approaches: A review," *IEEE Access*, vol. 8, pp. 93155–93178, 2020. http://dx.doi.org/10.1109/ACCESS.2020.2990528

[12] J. Hendriks, P. Dumond, and D. Knox, "Towards better benchmarking using the CWRU bearing fault dataset," *Mechanical Systems and Signal Processing.*, vol. 169, 2022. https://doi.org/10.1016/j.ymssp.2021.108732

[13] H. Abburi et al., "A closer look at bearing fault classification approaches," in *Proceedings of the Annual Conference of the PHM Society 2023.*, vol. 15, 2023. https://doi.org/10.48550/arXiv.2309.17001 J.

[14] J. Shen, S. Li, F. Jia, H. Zuo, and J. Ma, "A deep multi-label learning framework for the intelligent fault diagnosis of machines," *IEEE Access*, vol. 8, pp. 113557–113566, 2020. http://dx.doi.org/10.1109/ACCESS.2020.3002826

[15] C. Yu et al., "Multi-label fault diagnosis of rolling bearing based on meta-learning," *Neural Computing and Applications.*, vol. 33, pp. 5393–5407, 2021. https://doi.org/10.1007/s00521-020-05345-0 J.

[16] Z. Chen, A. M. Mauricio, W. Li, and K. Gryllias, "Multi-label fault diagnosis based on convolutional neural network and cyclic spectral coherence," in *HAL open science*, 2019, pp. 740. https://hal.science/hal-02188570v1

[17] Y. Jin et al., "Actual bearing compound fault diagnosis based on active learning and decoupling attentional residual network," *Measurement*, vol. 173, 2021. https://doi.org/10.1016/j.measurement.2020.108500

[18] S. Rajabi, M. S. Azari, S. Santini, and F. Flammini, "Fault diagnosis in industrial rotating equipment based on permutation entropy, signal processing and multi-output neuro-fuzzy classifier," *Expert Systems with Applications*, vol. 206, 2022. https://doi.org/10.1016/j.eswa.2022.117754

[19] J. Yang et al., "A novel based-performance degradation indicator RUL prediction model and its application in rolling bearing," *ISA Transactions*, vol. 121, pp. 349–364, 2022. https://doi.org/10.1016/j.isatra.2021.03.045

[20] S. Liu and L. Fan, "An adaptive prediction approach for rolling bearing remaining useful life based on multistage model with three-source variability," *Reliability Engineering & System Safety*, vol. 218, 2022. https://doi.org/10.1016/j.ress.2021.108182

[21] D.K. Saha et al., "Development of intelligent fault diagnosis technique of rotary machine element bearing: A machine learning approach," *Sensors*, vol. 22, p. 1073, 2022. https://doi.org/10.3390/s22031073

[22] Y. Ding et al., "A novel time–frequency Transformer based on self–attention mechanism and its application in fault diagnosis of rolling bearings," *Mechanical Systems and Signal Processing*, vol. 168, 2022. https://doi.org/10.1016/j.ymssp.2021.108616

[23] C. Lu et al., "Fault diagnosis of rotary machinery components using a stacked denoising autoencoder-based health state identification," *Signal Processing*, vol. 130, pp. 377–388, 2017. https://doi.org/10.1016/j.sigpro.2016.07.028

[24] T. Zhang et al., "A novel feature adaptive extraction method based on deep learning for bearing fault diagnosis," *Measurement*, vol. 185, 2021. https://doi.org/10.1016/j.measurement.2021.110030

[25] M. Alonso-González et al., "Bearing fault diagnosis with envelope analysis and machine learning approaches using CWRU dataset," *IEEE Access*, vol. 11, pp. 57796–57805, 2023. https://doi.org/10.1109/ACCESS.2023.3283466

[26] H. Tian, H. Fan, M. Feng, R. Cao, and D. Li, "Fault diagnosis of rolling bearing based on HPSO algorithm optimized CNN-LSTM neural network," *Sensors*, vol. 23, p. 6508, 2023. https://doi.org/10.3390/s23146508

[27] H. Sun and S. Zhao, "Fault diagnosis for bearing based on 1DCNN and LSTM," *Shock and Vibration*, vol. 2021, Art. no. 1221462, 2021. https://doi.org/10.1155/2021/1221462

[28] T. Ince, J. Malik, O. C. Devecioglu, S. Kiranyaz, O. Avci, L. Eren, and M. Gabbouj, "Early bearing fault diagnosis of rotating machinery by 1D self-organized operational neural networks," *IEEE Access*, vol. 9, pp. 139260–139270, 2021. https://doi.org/10.1109/ACCESS.2021.3117603

[29] R. N. Toma, F. Piltan, K. Im, D. Shon, T. H. Yoon, D. S. Yoo, and J. M. Kim, "A bearing fault classification framework based on image encoding techniques and a convolutional neural network under different operating conditions," *Sensors*, vol. 22, p. 4881, 2022. https://doi.org/10.3390/s22134881

[30] J. Yang, J. Liu, J. Xie, C. Wang, and T. Ding, "Conditional GAN and 2-D CNN for bearing fault diagnosis with small samples," *IEEE Transactions on Instrumentation and Measurement.*, vol. 70, Art. no. 5824912, 2021. https://doi.org/10.1109/TIM.2021.3119135

[31] A. P. Patil, B. K. Mishra, and S. P. Harsha, "Fault diagnosis of rolling element bearing using autonomous harmonic product spectrum method," *Proceedings of the Institution of Mechanical Engineers Part K Journal of Multi-body Dynamics*, vol. 235, no. 3, pp. 396–411, Jul. 2021. http://dx.doi.org/10.1177/1464419321994986

[32] A. S. Barcelos and A. J. Marques Cardoso, "Current-based bearing fault diagnosis using deep learning algorithms," *Energies (Basel)*, vol. 14, no. 9, 2021. https://doi.org/10.3390/en14092509

[33] H. S. Munir, S. Ren, M. Mustafa, C. N. Siddique, and S. Qayyum, "Attention-based GRU-LSTM for software defect prediction," *PLoS ONE*, 2021. https://doi.org/10.1371/journal.pone.0247444

[34] S. Xie, Y. Li, H. Tan, R. Liu, and F. Zhang, "Multi-scale and multi-layer perceptron hybrid method for bearings fault diagnosis," *http://dx.doi.org/10.1177/1464419321994986*, 2022. https://doi.org/10.1016/j.ijmecsci.2022.107708

[35] S. Li, H. Chen, Y. Chen, Y. Xiong, and Z. Song, "Hybrid method with parallel-factor theory, a support vector machine, and particle filter optimization for intelligent machinery failure identification," *Machines*, vol. 11, no. 8, p. 837, 2023. https://doi.org/10.3390/machines11080837

[36] L. Xia, P. Zheng, J. Li, W. Tang, and X. Zhang, "Privacy-preserving gradient boosting tree: Vertical federated learning for collaborative bearing fault diagnosis," *IET Collab. IET Collaborative Intelligent Manufacturing*, 2022. https://doi.org/10.1049/cim2.12057

[37] A. N. Saberi, A. Belahcen, J. Sobra, and T. Vaimann, "LightGBM-based fault diagnosis of rotating machinery under changing working conditions using modified recursive feature elimination," *IEEE Access*, vol. 10, pp. 81910–81925, 2022. https://doi.org/10.1109/ACCESS.2022.3195939

[38] S. Kiranyaz et al., "Zero-shot motor health monitoring by blind domain transition," *Mechanical Systems and Signal Processing*, vol. 210, p. 111147, 2024. https://doi.org/10.1016/j.ymssp.2024.111147

[39] W. A. Smith and R. B. Randall, "Rolling element bearing diagnostics using the case western reserve university data: A benchmark study," *Mechanical Systems and Signal Processing*, vols. 64–65, pp. 100–131, Dec. 2015. https://doi.org/10.1016/j.ymssp.2015.04.021

[40] H. Zheng et al., "Cross-domain fault diagnosis using knowledge transfer strategy: A review," *IEEE Access*, vol. 7, pp. 129260–129290, 2019. https://doi.org/10.1109/ACCESS.2019.2939876

[41] Konstruktions–Und Antriebstechnik (KAt)—Data Sets and Download (Universität Paderborn). Accessed: Dec. 22, 2019. [Online]. Available: https://mb.uni-paderborn.de/kat/forschung/datacenter/bearing-datacenter

[42] G. Geetha and P. Geethanjali, "An efficient method for bearing fault diagnosis," *Systems Science & Control Engineering*, vol. 12, no. 1, p. 2329264, 2024. https://doi.org/10.1080/21642583.2024.2329264

[43] *Apparatus & Procedures | Case School of Engineering | Case Western Reserve University*. Accessed: Apr. 4, 2024. [Online]. Available: https://engineering.case.edu/bearingdatacenter/apparatus-and-procedures

[44] T. Liang, S. Wu, W. Duan, and R. Zhang, "Bearing fault diagnosis based on improved ensemble learning and deep belief network," *Journal of Physics: Conference Series*, vol. 1074, Sep. 2018, Art. no. 012154. http://dx.doi.org/10.1088/1742-6596/1074/1/012154

[45] R. Zhang, Z. Peng, L. Wu, B. Yao, and Y. Guan, "Fault diagnosis from raw sensor data using deep neural networks considering temporal coherence," *Sensors*, vol. 17, no. 3, p. 549, 2017. https://doi.org/10.3390/s17030549

[46] S. Haidong, J. Hongkai, L. Xingqiu, and W. Shuaipeng, "Intelligent fault diagnosis of rolling bearing using deep wavelet auto-encoder with extreme learning machine," *Knowledge-Based Systems*, vol. 140, pp. 114, Jan. 2018. https://doi.org/10.1016/j.knosys.2017.10.024

[47] W. Zhang, G. Peng, C. Li, Y. Chen, and Z. Zhang, "A new deep learning model for fault diagnosis with good anti-noise and domain adaptation ability on raw vibration signals," *Sensors*, vol. 17, no. 2, p. 425, 2017. https://doi.org/10.3390/s17020425

[48] W. Mao, Y. Liu, L. Ding, and Y. Li, "Imbalanced fault diagnosis of rolling bearing based on generative adversarial network: A comparative study," *IEEE Access*, vol. 7, pp. 95159–9530, 2019. https://doi.org/10.1109/ACCESS.2018.2890693